



## PRÉDICTION DE L'AMPLIFICATION SISMIQUE À L'AIDE DE LA BASE DE DONNÉES KIK-NET AU JAPON

### SEISMIC AMPLIFICATION PREDICTION USING THE KIK-NET DATABASE IN JAPAN

Réception : 29/11/2023

Acceptation : 30/11/2023

Publication : 04/01/2024

BENMANSOUR Chohra<sup>1</sup>, DERRAS Boumédiène<sup>2</sup>

<sup>1</sup>Risk Assessment and Management Laboratory (RISAM), Abou Bekr Belkaïd University, BP 230, 13048, Chetouane, Tlemcen, Algeria.

[chohra.benmansour@univ-tlemcen.dz](mailto:chohra.benmansour@univ-tlemcen.dz)

<sup>2</sup>Department of Civil engineering and Hydraulics, Dr Moulay Tahar University, BP 138, 20000, Ennasr, Saida, Algeria.

[b\\_derras@mail.univ-tlemcen.dz](mailto:b_derras@mail.univ-tlemcen.dz)

**Résumé** - Le but de cette étude est de tester la sensibilité de l'amplification du site à différents indicateurs de l'état du site (SCPs) et à différentes mesures de l'intensité du mouvement du sol (GMIMs). La partie linéaire est représentée par trois vitesses d'ondes de cisaillement ( $V_{SX}$ ), où X correspond à 30, 50 et 100 m, l'effet non linéaire est pris en compte par  $PGV_2/V_{S30}$ , l'accélération maximale du site (PGA) et la vitesse maximale du site (PGV) représente la vitesse maximale du site. Pour réaliser ce test, nous développons un modèle de prédiction de l'amplification sismique basé sur la régression multiple. À cet égard, nous utilisons un ensemble de données composé d'un sous-ensemble de 977 enregistrements de la base de données KiK-Net pour les tremblements de terre de la croûte terrestre. Le modèle développé fournit le facteur d'amplification du site (AF) pour des périodes allant de 0,01 à 4,00 s. L'utilisation de  $[V_{S30} PGV_2/V_{S30}]$  permet d'obtenir l'écart-type le plus faible (sigma) et le coefficient de réduction de la variance le plus élevé  $R_c$  (%), tout en respectant le comportement physique sous-jacent.

**Mots - clés** : Amplification du site, SCPs, Régression multiple, Écart-type, KiK-Net.

**Abstract**-The aim of this study is to test the sensitivity of site amplification to different site condition proxies (SCPs) and ground motion intensity measures (GMIMs). The linear part is represented by three shear wave velocities ( $V_{SX}$ ), where the X corresponds to 30, 50 and 100 m, the nonlinear effect is taking care of by  $PGV_2/V_{S30}$ , the maximum site acceleration (PGA), and the maximum site velocity (PGV) represents the maximum site velocity. To perform this test, we develop a seismic amplification prediction model based on multiple regression. In this regard, we use a dataset consisting of a subset of 977 records from the KiK-Net database for crustal earthquakes. The model developed provides the site amplification factor (AF) for periods ranging from 0.01 to 4.00 s. the use of  $[V_{S30} PGV_2/V_{S30}]$  provides the lowest standard deviation (sigma) and the highest variance reduction coefficient  $R_c$  (%), while respecting the underlying physical behavior.

**Keywords**: Site amplification, SCPs, Multiple regression, Standard deviation, KiK-Net.

## 1-Introduction

The assessment of site effects relies on understanding the geological and geometric characteristics of soil layers. However, acquiring such information can be costly, particularly for deep soil configurations. To address this, researchers have explored the use of site condition proxies (SCPs) [1], [2], as well as Ground Motion Intensity Measures (GMIMs) that account for the nonlinear behavior of soil [3]–[5].

This paper aims to examine the impact of SCPs and GMIMs on the amplification factor. The analysis involves assessing the standard deviation figures and the improvement achieved in calculating the reduction coefficient. The regression method is employed to combine the most effective SCP and GMIM.

Following a brief introduction of the dataset, the paper dedicates a section to present the regression models developed. Subsequently, the results obtained from the KiK-net data are discussed, with a focus on evaluating the performance of individual site condition proxies and Ground Motion Intensity Measures, both separately and in combination.

## 2- DATA

The Kiban–Kyoshin network (KiK-net) was established in Japan after the 1995 Kobe earthquake as one of the two national strong-motion seismograph networks. It consists of approximately 700 stations strategically distributed across the Japanese islands with an average spacing of about 20 km [6]. Each KiK-net station is equipped with a pair of surface and downhole, sensitive three-component digital accelerometers, enabling the empirical evaluation of site response at each location. The dataset used in this study was compiled by [7].

The dataset includes 977 recordings from 199 sites, capturing seismic activity from 214 earthquakes. Table 1 presents the range of magnitudes ( $M_w$ ), distances from the rupture area ( $R_{JB}$ ), depths, as well as the values for the SCPs ( $V_{S30}$ ,  $V_{S50}$ ,  $V_{S100}$ ) and GMIMs (PGA, PGV,  $PGV_2/V_{S30}$ ). The table also provides the corresponding number of earthquakes, records, and

sites. Notably, the recorded PGA values range from  $2.6 \times 10^{-4}$  to 0.41 g.

**Table 1:** the range of metadata parameters accompanied with the number of earthquakes, recordings and site

**Tableau 1:** la gamme de paramètres de métadonnées accompagnés du nombre de tremblements de terre, d'enregistrements et de sites

Metadata Parameter	Parameter Range	Total Number of Earthquakes	Total Number of Recordings	
	Min	Max	214	977
$M_w$	3.7	6.9		
$R_{JB}$ (Km)	3.65	440.62	5	
Focal Depth (Km)	0	30		
$V_{S30}$ (m/s)	152.94	1432.7	5	
$V_{S50}$ (m/s)	210	1622.9	4	
$V_{S100}$ (m/s)	305.45	2087.3	1	
PGA (g)	0.00026	0.413	8	
PGV (m/s)	0.0013	0.208		
$PGV_2/V_{S30}$	$1.5 \times 10^{-7}$	0.0013		

### 2.1- DATA DISTRIBUTION

In order to examine the potential correlation between  $V_{S30}$  and the selected GMIMs, a Correlation Coefficient was calculated (see figure 1). The analysis reveals that the weakest correlation ( $R = 0.05$ ) was observed between  $V_{S30}$  and PGV. On the other hand, the strongest correlation was found between  $V_{S30}$  and  $PGV_2/V_{S30}$  with  $R = 0.26$ , these results indicate that there is no significant dependency between  $V_{S30}$  and GMIMs.

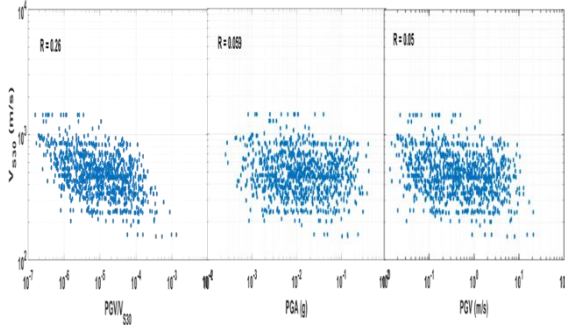


**Figure 1 :** The Correlation Coefficient of  $V_{S30}$  VS  $PGV_2/V_{S30}$ , PGA and PGV.

**Figure 1 :** Coefficient de corrélation entre  $V_{S30}$  VS  $PGV_2/V_{S30}$ , PGA et PGV.

### 3-METHODOLOGY

In this study, the multiple regression technique is employed to estimate the Amplification Factor. Various researchers have proposed different equations known as Ground Motion Prediction Equations (GMPEs), which incorporates all relevant effects, including Source, Path, and Site [8]–[10]. Some of these models also include nonlinear effects [11]–[13]. However, The models developed in these studies use a single site characterization parameter (SCP).

In our model, we introduce a combination that relates the Amplification Factor (as the independent variable) with one SCP and one Ground Motion Intensity Measure (GMIM) (as the dependent variables). Thus, the final equation can be expressed as follows :

$$\text{Log}_{10}(\text{AF}(T)) = a + b \cdot \text{log}_{10}(V_{S30}) + c \cdot \text{log}_{10}(PGV_2/V_{S30}) \quad (1)$$

### 4- RESULTS

In this section, we will discuss the Standard Deviation values. Figure 2 illustrates the variation of Site Characterization Parameters (SCPs) ( $V_{S30}$ ,  $V_{S50}$ ,  $V_{S100}$ ) across different Periods. A preliminary analysis reveals distinct behavior among the three models across various Period ranges. Specifically,  $V_{S100}$  exhibits the best performance in the short Period interval (0.01-0.1s), while  $V_{S30}$  outperforms the others in the intermediate range (0.1-0.4s). In the remaining Period range,  $V_{S50}$  emerges as the most dominant.

Based on these observations, we have chosen  $V_{S30}$  as the preferred SCP for our study. This decision is primarily influenced by cost considerations, as  $V_{S30}$  is comparatively more affordable than the other two SCPs.

$$\sigma = \sqrt{\frac{1}{N} \sum (AF - \bar{AF})^2} \quad (2)$$

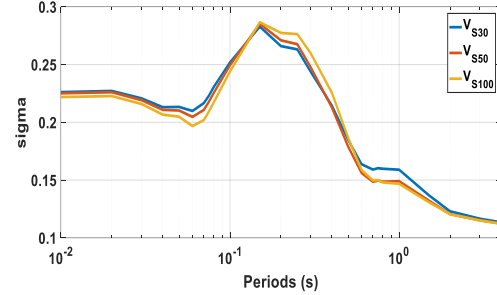


**Figure 2 :** The variation of SCPs VS Periods.

**Figure 2 :** la variation des SCPs VS Périodes.

Figure 3 presents the analysis of Ground Motion Intensity Measures (GMIMs) in the same study. Among the GMIMs considered,  $PGV_2/V_{S30}$  is considered to be the best GMIM in the entire range, reaching a peak of 0.28 at  $T = 0.15$ . Based on the results of Figure 2 and 3, we made the decision to create a new combination of [ $V_{S30}$   $PGV_2/V_{S30}$ ] in order to evaluate the gain obtained by this combination.

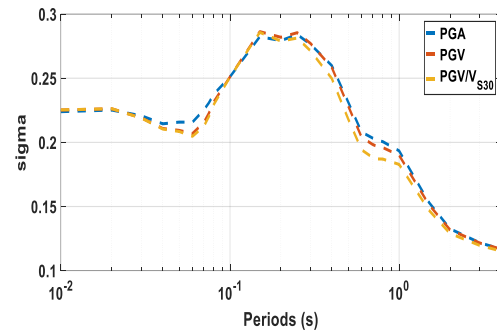


**Figure 3 :** The variation of GMIMs VS Periods.

**Figure 3 :** la variation des GMIMs VS Périodes.

To gain a better knowledge, we calculate the Reduction Coefficient

$$R_C(\%) = \left(1 - \frac{\sigma \log_{10}(\text{AF})_{\text{model}}^2}{\sigma \log_{10}(\text{AF})_{\text{database}}^2}\right) \times 100 \quad (3)$$

The results are presented in Figure 4, where three models were developed: SCP only,

GMIM only, and the combination of SCP with GMIM ([SCP GMIM]). Among the three models, [SCP GMIM] proves to be the most effective across the entire range, the combined model demonstrates a 3% improvement compared to the SCP alone. On the other hand, the worst performing model is the one using  $PGV_2/V_{S30}$  alone.

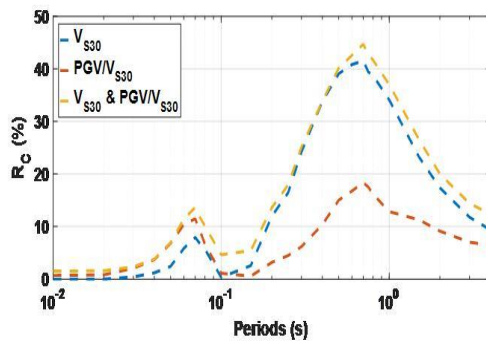


**Figure 4 :** The variation of SCPs and GMIMs when they are alone and combined.

**Figure 4 :** la variation des SCPs et GMIMs lorsqu'ils sont seuls et combinés.

Following a series of tests, a new combination has been established and the next step involves examining its trend. Figure 5 displays the trend of the model based on 50% of the Cumulative Distribution Function (CDF), with specific values of  $V_{S30} = 468$  m/s and  $PGV_2/V_{S30} = 9.2 \cdot 10^{-6}$ . The curve exhibits a smooth and evolving behavior. It begins with a stable segment between 0.01-0.04s, followed by an increasing part that reaches a peak value of 6.7 at  $T = 0.1$ s. Subsequently, a decreasing segment is observed.

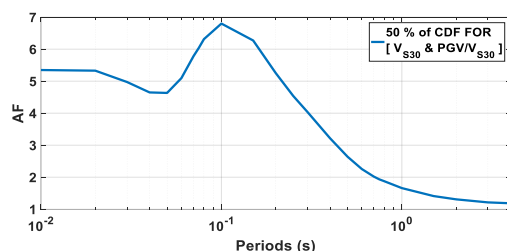


**Figure 5 :** The Amplification Factor for  $[V_{S30} PGV_2/V_{S30}]$  when CDF = 50 %.

**Figure 5 :** Le Facteur d'amplification pour  $[V_{S30} PGV_2/V_{S30}]$  quand CDF = 50 %.

## 5- DISCUSSION OF RESULTS

In this study, we tested the sensitivity of site amplification using different site condition proxies (SCPs) and ground motion intensity measures (GMIMs). We developed a seismic amplification prediction model based on multiple regression technique, we used a subset of 977 records from the KiK-Net database for crustal earthquakes.

The results showed that the combination  $[V_{S30} PGV_2/V_{S30}]$  was the most suitable, exhibiting the lowest standard deviation and the highest variance reduction coefficient. " $V_{S30}$ " proved to be the best SCP for representing site conditions, while " $PGV_2/V_{S30}$ " was optimal for representing ground motion intensity.

Our robust site amplification prediction model based on multiple regression technique demonstrated consistent performance for different periods from 0.01 to 4.00 seconds, with smooth transitions between different parts of the period spectrum

## 6- CONCLUSION

In conclusion, this work utilized a subset of the KiK-net database to determine the most suitable combination for representing the dataset. Regression analysis was performed, linking the Amplification Factor (AF) with Site condition Proxy (SCP) and Ground Motion Intensity Measure (GMIM). Based on several tests conducted, here are some highlights:

- The analysis of Standard Deviation figures (Figure 2 & 3) indicates that  $V_{S30}$  is the preferred SCP, while  $PGV_2/V_{S30}$  is the optimal GMIM
- The Reduction Coefficient figure (Figure 4) demonstrates that the newly introduced combination  $[V_{S30} PGV_2/V_{S30}]$  outperforms the individual use of SCP or GMIM.
- The predicted Amplification Factor by the new combination exhibits smooth behavior with different transition parts.
- However, there is room for improvement in the  $[V_{S30} PGV_2/V_{S30}]$  combination by incorporating an

additional SCP that is sensitive to low Period range.

- These results highlight the effectiveness of the chosen combination and suggest ways of improving Prediction accuracy.

## RÉFÉRENCES BIBLIOGRAPHIQUES

- [1] Y. Choi and J. P. Stewart, “Nonlinear Site Amplification as Function of 30 m Shear Wave Velocity,” *Earthq. Spectra*, vol. 21, no. 1, pp. 1–30, Feb. 2005, doi: 10.1193/1.1856535.
- [2] L. Luzi, R. Puglia, F. Pacor, M. R. Gallipoli, D. Bindi, and M. Mucciarelli, “Proposal for a soil classification based on parameters alternative or complementary to  $V_s$ ,30,” *Bull. Earthq. Eng.*, vol. 9, no. 6, pp. 1877–1898, Dec. 2011, doi: 10.1007/s10518-011-9274-2.
- [3] B. Derras, P. Y. Bard, and F. Cotton, “VS30, slope, H800 and  $f_0$ : Performance of various site-condition proxies in reducing ground-motion aleatory variability and predicting nonlinear site response 4. Seismology,” *Earth, Planets Sp.*, vol. 69, no. 1, Dec. 2017, doi: 10.1186/s40623-017-0718-z.
- [4] B. Derras, P. Y. Bard, J. Régnier, and H. Cadet, “Non-linear modulation of site response: Sensitivity to various surface ground-motion intensity measures and site-condition proxies using a neural network approach,” *Eng. Geol.*, vol. 269, no. January, 2020, doi: 10.1016/j.enggeo.2020.105500.
- [5] J. Regnier, H. Cadet, L. F. Bonilla, E. Bertrand, and J.-F. Semblat, “Assessing Nonlinear Behavior of Soils in Seismic Site Response: Statistical Analysis on KiK-net Strong-Motion Data,” *Bull. Seismol. Soc. Am.*, vol. 103, no. 3, pp. 1750–1770, Jun. 2013, doi: 10.1785/0120120240.
- [6] T. Hayashida and F. Tajima, “Calibration of amplification factors using KiK-net strong-motion records: Toward site effective estimation of seismic intensities,” *Earth, Planets Sp.*, vol. 59, no. 10, pp. 1111–1125, 2007, doi: 10.1186/BF03352054.
- [7] H. M. Dawood, A. Rodriguez-Marek, J. Bayless, C. Goulet, and E. Thompson, “A Flatfile for the KiK-net Database Processed Using an Automated Protocol,” *Earthq. Spectra*, vol. 32, no. 2, pp. 1281–1302, May 2016, doi: 10.1193/071214eqs106.
- [8] B. S.-J. Chiou and R. R. Youngs, “Update of the Chiou and Youngs NGA Model for the Average Horizontal Component of Peak Ground Motion and Response Spectra,” *Earthq. Spectra*, vol. 30, no. 3, pp. 1117–1153, Aug. 2014, doi: 10.1193/072813EQS219M.
- [9] L. Kang and J. X. Zhao, “Ground-Motion Prediction Equations for Shallow-Crustal and Upper-Mantle Earthquakes in Japan Using Site Class and Segmented Geometric Attenuation Functions for the Horizontal Component,” *Bull. Seismol. Soc. Am.*, vol. 112, no. 3, pp. 1502–1526, Jun. 2022, doi: 10.1785/0120200383.
- [10] J. X. Zhao *et al.*, “Ground-motion prediction equations for shallow crustal and upper-mantle earthquakes in Japan using site class and simple geometric attenuation functions,” *Bull. Seismol. Soc. Am.*, vol. 106, no. 4, pp. 1552–1569, Aug. 2016, doi: 10.1785/0120150063.
- [11] E. Kalkan, “Prepared in cooperation with the U . S . Nuclear Regulatory Commission Update of the Graizer – Kalkan Ground - Motion Prediction Equations for Shallow Crustal Continental Earthquakes By Vladimir Graizer and Erol Kalkan,” no. January, 2015.
- [12] M. A. Sandıkkaya, “On linear site amplification behavior of crustal and subduction interface earthquakes in Japan: (1) regional effects, (2) best proxy selection,” *Bull. Earthq. Eng.*, vol. 17, no. 1, pp. 119–139, 2019, doi: 10.1007/s10518-018-0459-9.
- [13] J. X. Zhao *et al.*, “Nonlinear Site Models Derived from 1D Analyses for Ground-Motion Prediction Equations Using Site Class as the Site Parameter,” *Bull. Seismol. Soc. Am.*, vol. 105, no. 4, pp. 2010–2022, Aug. 2015, doi: 10.1785/0120150019.